

LA-UR-08-4668

Approved for public release;  
distribution is unlimited.

*Title:* A Code Comparison Study for the Bigten Critical Assembly

*Author(s):* Robert E. MacFarlane, T-16  
Roger M. Blomquist, Argonne Nat. Lab.  
Dermott E. Cullen, Edward Lent, Livermore Nat. Lab.  
Jean Christophe Sublet, CEA, DEN, Cadarache, France

*Intended for:* General Distribution



Los Alamos National Laboratory, an affirmative action/equal opportunity employer, is operated by the Los Alamos National Security, LLC for the National Nuclear Security Administration of the U.S. Department of Energy under contract DE-AC52-06NA25396. By acceptance of this article, the publisher recognizes that the U.S. Government retains a nonexclusive, royalty-free license to publish or reproduce the published form of this contribution, or to allow others to do so, for U.S. Government purposes. Los Alamos National Laboratory requests that the publisher identify this article as work performed under the auspices of the U.S. Department of Energy. Los Alamos National Laboratory strongly supports academic freedom and a researcher's right to publish; as an institution, however, the Laboratory does not endorse the viewpoint of a publication or guarantee its technical correctness.

# A Code Comparison Study for the Bigten Critical Assembly

*by*

Robert E. MacFarlane (Los Alamos National Laboratory)  
Roger M. Blomquist (Argonne National Laboratory)  
Dermott E. Cullen (Lawrence Livermore National Laboratory)  
Edward Lent (Lawrence Livermore National Laboratory)  
Jean Christophe Sublet (CEA, DEN, Cadarache, France).

## *Abstract*

The performance of six popular continuous-energy Monte Carlo and multigroup transport codes has been compared for a simple spherical model of the Bigten critical assembly using ENDF/B-VII nuclear data. This “code comparison” exercise was supplemented with a few “data testing” results using different nuclear data evaluations. This particular critical assembly was chosen because it is sensitive to the U-238 unresolved resonance range, thus extending recent good results obtained for faster criticals like Godiva and Jezebel. After some improvements, the results showed generally good agreement between the codes, their differences being generally smaller than the differences between those seen when using different evaluated data libraries. This suggests that the current generation of codes is adequate for studying assemblies similar to Bigten and for evaluating the effects of possible improvements in the nuclear data libraries.

## **Introduction**

There has been a significant improvement in our capabilities to predict nuclear criticality in recent years. This has been due to three factors: (1) improved nuclear data evaluation sets, such as ENDF/B-VII [1], JEFF-3.1 [2], and JENDL-3.3 [3]; (2) high-quality nuclear simulation codes based on continuous-energy Monte Carlo methods, such as MCNP [4], TART [5], TRIPOLI [6], VIM [7], and COG [8]; and (3) the availability of reliable models for benchmark critical assemblies in the International Handbook of Evaluated Criticality Safety Benchmark Experiments [9] (the ICSBEP Handbook). Because of this improvement, nuclear data evaluators have begun to pay attention to processes that lead to smaller and smaller effects on calculated criticality. This showed up in the development of the ENDF/B-VII library, where attempts were made to decide between various options that led to effects on criticality ( $K$ -eff) on the order of 0.1%. Clearly, these kinds of judgments would be unfounded if there were differences in the simulation codes and their data generation methods that lead to differences larger than 0.1%!

At this point, it is useful to try to distinguish between “data testing” and “code comparison testing.” In the latter, one tries to find (and remove) differences between the various simulation codes and their processing methods by running the same problems using the same data source. In data testing, one runs the problems using data from different evaluation sets and compares to experiment. Clearly, to really test the data to some desired accuracy, the simulation codes must be consistent to about that accuracy based on the results of code comparison testing.

This report is intended to be a contribution to “code comparison testing.” We have all agreed to use data based on the ENDF/B-VII library to run a common criticality problem with different simulation codes and data processing methods. In another recent code comparison exercise [10], the LANL and LLNL authors did a study of how our various codes performed for the simple, spherical, fast critical assemblies Godiva, Jezebel, and Jezebel23. That study enabled us to identify several differences between the codes, and the end results were reasonably good. We now want to extend the study to lower energies that feature the complexities associated with the unresolved resonance range and to include more participants. The best candidate systems would be critical assemblies containing lots of U-238, because its relatively narrow and widely spaced resonances give a strong unresolved self shielding effect. In addition, the previous study provided some checks on how U-235, Pu-239, and U-233 performed in our codes. This study would extend that to check on the performance of U-238 for keV and higher energies.

We chose to use the simple spherical model for Bigten from the US Cross Section Evaluation Working Group (CSEWG) data testing set [11] for most of the comparisons. Its simplicity and symmetry makes it easier to compare results from various codes and give multigroup codes a fair chance to compare well to Monte Carlo codes. This model was constructed by the original Bigten experimenters at Los Alamos. For our study, we added a small central region for recording flux and reaction rates, because the Bigten model provides some experimental results for fission, capture, and activation ratios. The radii of the three regions are

1.5, 30.48, and 45.72 cm

There are two materials, the core composition in regions 1 and 2, and the reflector composition in region 3:

Core composition (atoms per barn-cm): U-235 4.84-3, U-238 4.268-2, U-234 5.0-5  
Reflector composition (atoms per barn-cm): U-235 1.0-4, U-238 4.797-2

The region material densities are

Core region: .04757 atoms per barn-cm or 18.7799 g/cc  
Reflector region: .04807 atoms per barn-cm or 19.0015 g/cc

Integral results were requested to enable the following system total results to be calculated: flux; production as a sum of fission production, (n,2n) production, and (n,3n)

production; absorption as a sum of fission, capture, (n,2n), and (n,3n); and leakage from the outer edge of the system. The normalization of these results is not important, because a reactor can be critical at any power level. In this study, all the results are renormalized so that the total production is unity. The system value of K-eff is then given by

$$K_{eff} = \frac{1}{\text{absorption} + \text{leakage}}$$

The model quotes a K-eff value of 0.996+/-0.003. Results from other more detailed models are given later in this report.

Details were to be provided using 616 groups or tally bins as defined in the Appendix (some runs used only the highest-energy 256 groups above 100 eV). These tally bins are logarithmic with 50 bins per decade. Results are tabulated using the tally scores in the bins, therefore fluxes and reaction rates are proportional to per lethargy values. When possible, it is desirable to have region-wise and total flux values for each bin. Region-wise and total collision rates are also useful. The main comparisons were intended to be on system-averaged production, absorption, and leakage values. These could be provided as region-wise values, if convenient, and they would be summed over regions for the comparisons. It was desirable to have fission production, (n,2n) production, and (n,3n) production either given separately, merged together, or given as (n,Xn) production and (n,Xn) loss. The total production would be normalized to unity, and that normalization factor would be used to renormalize the absorption and leakage for the comparison graphs.

Optional results could include isotopic reaction rates in the central region. These can be used to compute things like the U-238/U-235, Np-237/U-235, U-233/U-235, and Pu-239/U-235 fission ratios for comparison to the results provided with the model. The model also includes U-238 capture to U-235 fission ratio results, and there are activation ratios to U-235 fission for  $^{10}\text{B}(n,\alpha)$ ,  $^{27}\text{Al}(n,\alpha)$ ,  $^{45}\text{Sc}(n,\gamma)$ ,  $^{46}\text{Ti}(n,p)$ ,  $^{47}\text{Ti}(n,p)$ ,  $^{48}\text{Ti}(n,p)$ ,  $^{54}\text{Fe}(n,p)$ ,  $^{58}\text{Fe}(n,\gamma)$ ,  $^{58}\text{Ni}(n,p)$ ,  $^{59}\text{Co}(n,\gamma)$ ,  $^{63}\text{Cu}(n,\gamma)$ , and  $^{197}\text{Au}(n,\gamma)$ .

## Integral Results

Here are comparisons of the integral results from 5 different continuous-energy Monte Carlo codes. The absorption and leakage values are based on a normalization where the total production, including both fission and (n,Xn) processes, has been adjusted to unity. Therefore, K-eff is just equal to one over the sum of absorption and leakage.

For some of the codes, the problem was run without unresolved self shielding in order to highlight that effect. Note that including the self shielding leads to an increase in K-eff of about 0.35% (350 pcm) resulting mostly from reduced U-238 absorption.

**Table 1. Integral Results With Unresolved Resonance Self-Shielding**

	<b>Absorption</b>	<b>Leakage</b>	<b>K-eff</b>
Measurement			0.996+/-0.003
COG	.876983	.125390	0.99763
MCNP	.876444	.125880	0.99768
TART	.876536	.125633	0.99783
TRIPOLI	.875432	.126260	0.99831
VIM	.876523	.125853	0.99763

**Table 2. Integral Results Without Unresolved Resonance Self-Shielding**

	<b>Absorption</b>	<b>Leakage</b>	<b>K-eff</b>
MCNP	.884520	.121459	0.99406
TART	.884691	.121389	0.99402
TRIPOLI	.884657	.121288	0.99409

It is clear that the results for these 5 codes are in very good agreement, the total spread in K-eff in the first table being only 0.07%. The Monte Carlo runs were done using one billion histories, so the statistical uncertainty on the K-eff values is on the order of 0.00005. The spread in absorption values is about 0.2%, and the spread in the leakage values is about 0.7%.

The results with self shielding turned off are even closer, suggesting that most of the remaining differences in Table 1 are caused by differences in handling the unresolved energy range. Note that the net effect of including unresolved resonance self shielding is significant, leading to a change in K-eff on the order of 0.35% (350 pcm) in a direction to improve the agreement with experiment.

## **Flux and Reaction-Rate Comparisons**

Comparisons of system-averaged flux, production, absorption, and leakage are shown in Figures 1 through 4. These values were obtained from the diverse output listings of the various codes by extracting numbers, combining regions as needed, and renormalizing to the unity production standard. The integral over each curve is given in the legend block.

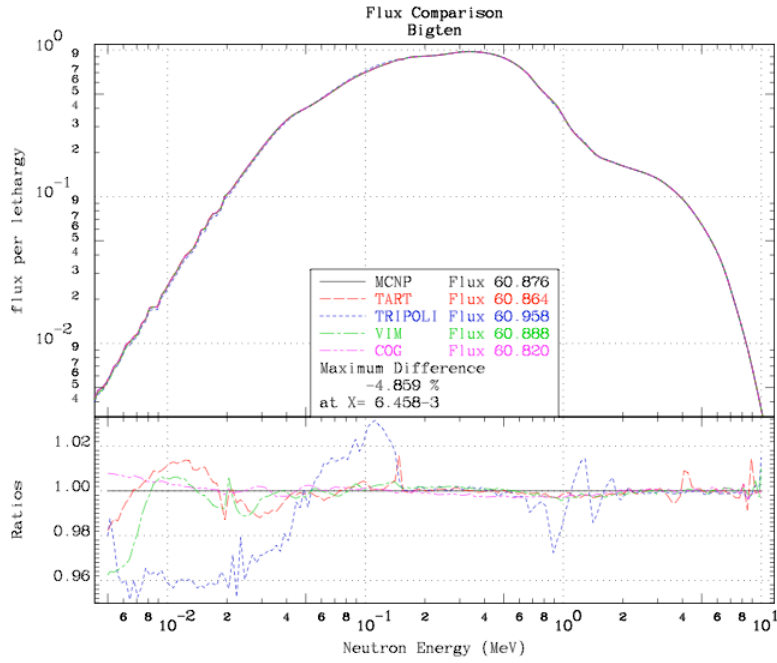


Figure 1. Comparison of system-averaged flux for 5 codes.

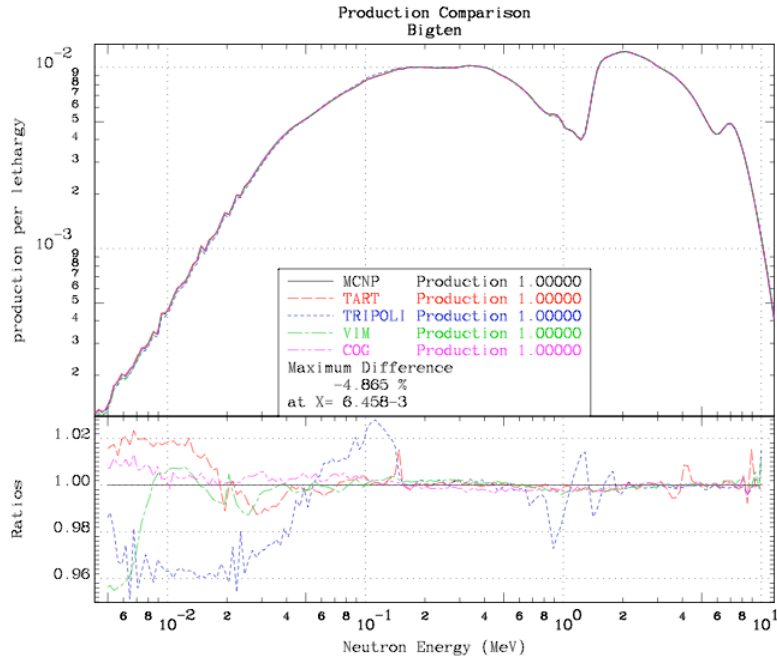
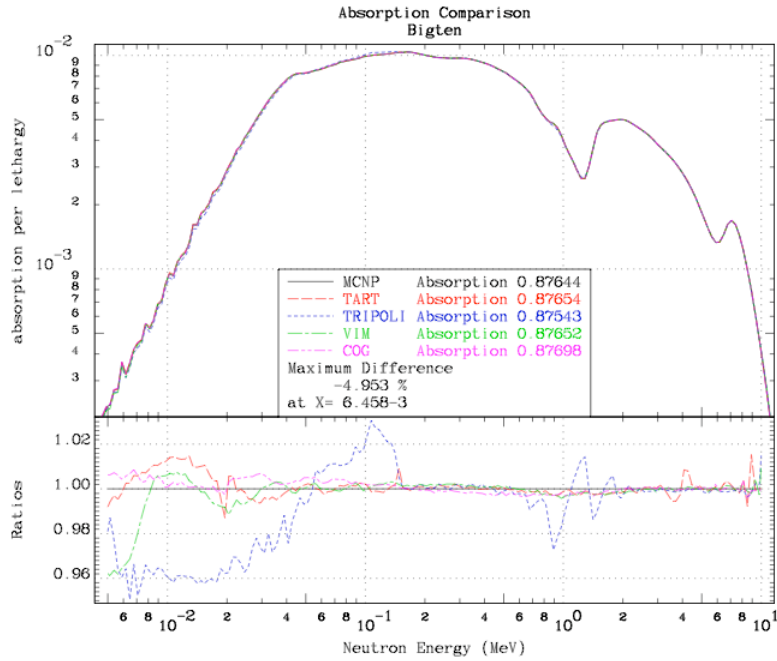
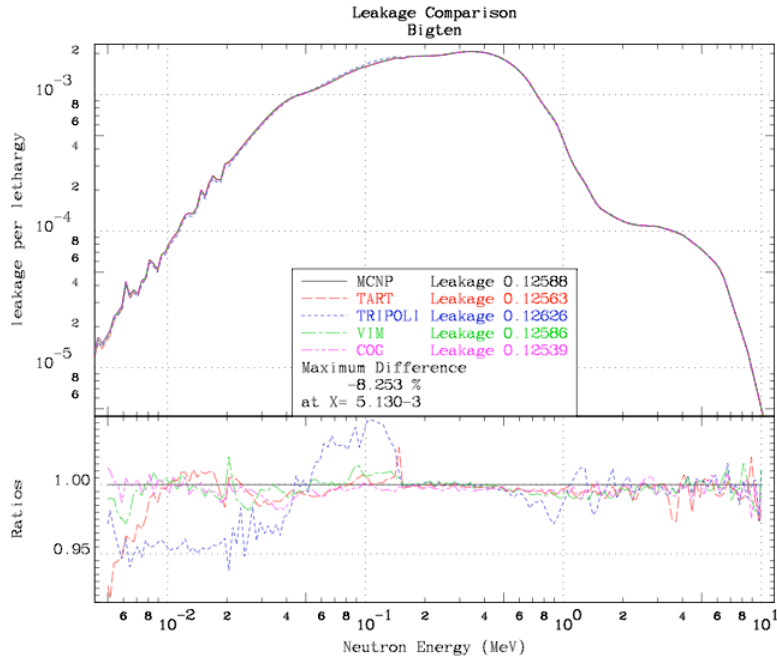


Figure 2. Comparison of system-averaged production for 5 codes.



**Figure 3. Comparison of system-averaged absorption for 5 codes.**



**Figure 4. Comparison of system leakage for 5 codes.**

These figures show that the agreement between MCNP, TART, COG, and VIM is very good, except for isolated differences. The TRIPOLI results differ below the upper limit of the U-238 unresolved range at 149 keV, probably because of a different treatment of the inelastic scattering that competes in the unresolved resonance range. TRIPOLI also shows a set of wiggles around 1 MeV. As discussed in more detail below, these are caused by the method used for incident-energy interpolation in continuum scattering distributions. There begins to be some additional divergence of the results at the lowest energies shown here, but this region is not very important to the integral results for Bigten. The sharp peaks at the edges of the U-238 unresolved resonance range (20 to 149 keV) for TART are due to the use of group averaged unresolved resonance parameters that overlap the boundaries of the unresolved range.

The initial results of this study showed slightly greater differences than these in some places. Some improvements were made in the inelastic scattering and unresolved resonance treatments for TART. The treatment of the high-threshold (n,3n) reaction was improved for TRIPOLI. These improvements illustrate the value of this kind of code comparison testing.

## **Effects of the Unresolved Resonance Range**

One of the reasons for carrying out this study was to validate the performance of the various codes for computing self shielding in the U-238 unresolved resonance range (20 to 149 keV). The Bigten system has enough flux in this region to make it relatively important for criticality. This effect was already demonstrated by Tables 1 and 2. To illustrate the effect in more detail, Figure 5 shows a comparison of MCNP and TRIPOLI run with the probability-table self shielding turned off to MCNP with UR self shielding turned on.

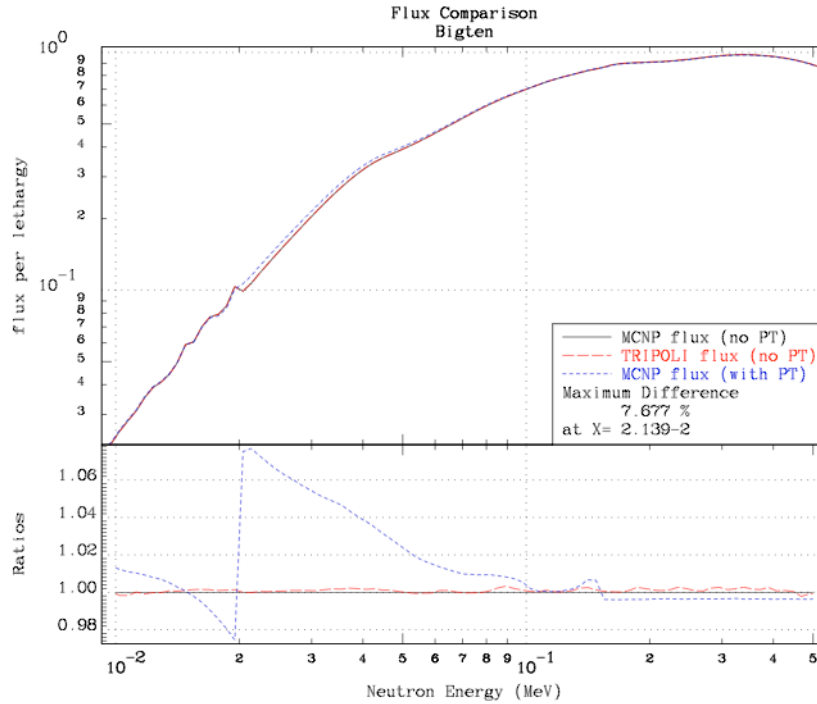


**Figure 5. Effect on Flux of Unresolved Resonance Range Self Shielding and Comparison of 2 Codes with Probability Tables Turned Off.**

Note that the TRIPOLI and MCNP fluxes agree fairly well in this plot when neither uses probability tables (PT). The larger deviations between the two codes seen in Figure 1 are absent. This implies that those deviations are a result of the way TRIPOLI treats unresolved inelastic scattering. It is somewhat different from the methods used in the other codes, in that TRIPOLI applies self shielding to the competing inelastic reaction through its use of CALENDF probability tables. The other codes do not (as specified by the ENDF procedures [12]).

Another way to compare these codes in the unresolved resonance region is to compute the ratios of collisions to flux and absorptions to flux; that is, the effective macroscopic total and absorption cross sections averaged over the system. The results of this comparison are shown in Figures 6 and 7.

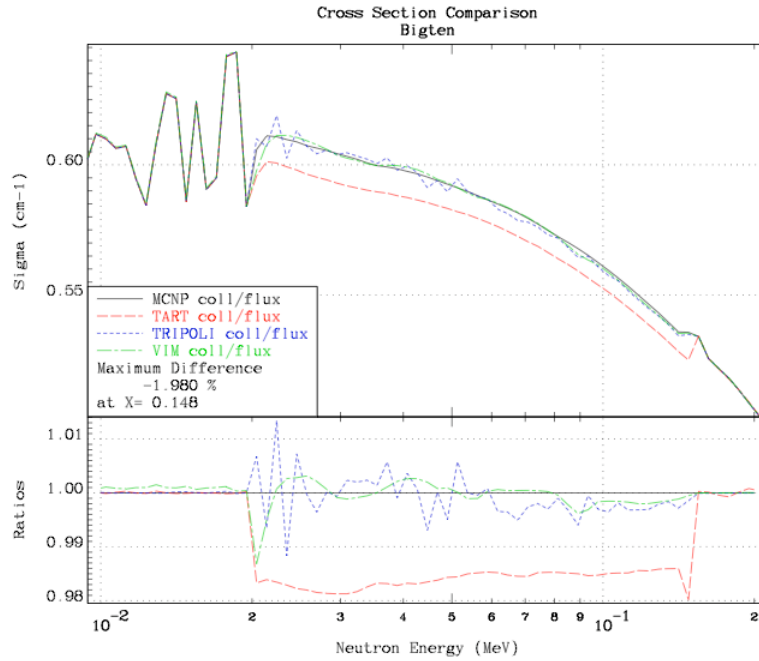


**Figure 6. Effective total cross section in Bigten for 4 codes.**

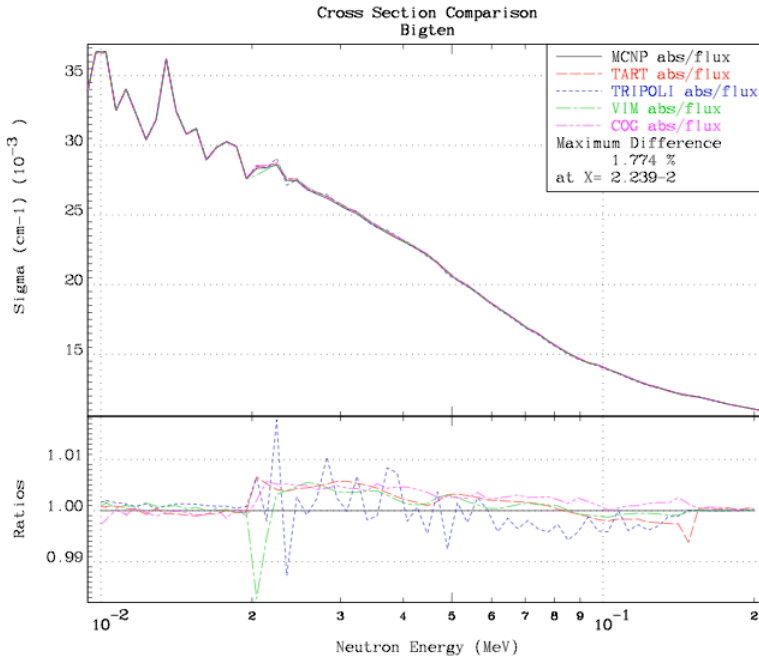


**Figure 7. Effective absorption cross section in Bigten for 5 codes.**

To understand the differences seen in Figures 6 and 7, it is useful to summarize the methods used for unresolved resonance self shielding in the various codes.

***Summary of Method Used for MCNP.*** The probability tables for MCNP are generated using the PURR module of NJOY [13]. For each energy given in the evaluation, the parameters for a long series (or “ladder”) of resonances are constructed using Wigner spacing for resonance centers and the chi-squared distributions from the evaluation for resonance widths. The code then randomly selects an energy in the range of the series and computes the cross sections at that point using Single-Level Breit-Wigner (SLBW) resonance shapes and psi-chi Doppler broadening. In the beginning, it does this for a number of random energies to get a rough idea of the distribution of the total cross section; it then analyzes this rough idea to construct a set of total cross section bins for the rest of the process (typically, 20 bins are used). It then returns to the first ladder and samples it with random energies. The resulting total cross sections are added to the appropriate bin in the probability table, and the conditional averages for scattering, fission, and capture are accumulated in the bin corresponding to the total cross section. The code then constructs a new ladder and repeats the sampling process. This is continued for the requested number of ladders (typically 32). For materials with the ENDF LSSF parameter set to zero, the table cross sections are renormalized to match the computed infinitely dilute values. For LSSF=1, the values in the table are converted to self shielding factors, and then MCNP multiplies these factors times the cross sections from the standard ENDF file to get the appropriate value. Note that there are no energy bounds (such as group bounds) in this process. Therefore, it computes cross sections that have basically the same smoothness as the unresolved resonance range evaluation.

***Summary of Method Used for TART (written by DEC).*** Like the other codes (MCNP, TRIPOLI) TART starts with randomly sampled ladders of resonances; TART uses as many ladders as it judges to be necessary to reach convergence. TART reconstructs the energy dependent cross sections (including competition), and Doppler broadens them, using the ENDF/B PREPRO codes, RECENT and SIGMA1 [14] It then uses the Multiband method [15], built into the ENDF/B PREPRO GROUPIE code [14], to calculate Bondarenko self-shielded cross sections, which are used to directly define Multiband parameters to handle self-shielding. TART defines Bondarenko self-shielded averages over small energy intervals, usually the TART 50 groups per energy decade representation.

In principle this should be more accurate than the other methods, because it does not randomly sample energies, and rather than using the psi-chi method, it uses exact SIGMA1 Doppler broadening. I expect this approach to produce slightly lower elastic minima, which means slightly lower self-shielded cross sections, which is exactly the result that we see in this report; see. Fig. 6.

In practice all of the methods are limited by ENDF/B only allowing single-level Breit-Wigner resonance parameters in the unresolved resonance region; to my eye this is a real weakness in the ENDF/B system. Over the last decades our treatment of the resolved

resonance region has improved immensely, with the addition of better resonance formalisms, such as Reich-Moore. In contrast the unresolved treatment has not been improved at all. So that today evaluators can do an excellent job in the resolved region, but then are forced to use less accurate methods in the unresolved region. The result can be inconsistency between the resolved and unresolved resonance regions and between the unresolved and fast regions.

The methods we are all using to handle the unresolved region are now 30 or 40 years old, and in my humble opinion it is time that the ENDF/B procedures be updated.

***Summary of Method Used for TRIPOLI.*** The probability tables for TRIPOLI are generated using CALENDF [16]. The code works with a set of energy groups defined across an energy range, in this the unresolved resonance range (URR). Based on the average resonance parameters and the required accuracy, CALENDF defines energy zones adapted to the group structure. If the group structure is coarse, several discontinuous zones are selected. If the structure is fine, a zone may cover several groups. Average parameters are computed for each zone using File 2 of the evaluation. Random ladders of resonances are generated with energies extracted from a table of 1185 values that are the eigenvalues of a random matrix (Dyson and Mehta) and with resonance widths chosen from the distribution laws with stratified and antithetic sampling. A few resonances are added below and above the range of the energy zone to handle edge effects.

The cross sections for each ladder are computed on a fine energy grid using the MNBW formalism (Multi Niveau Breit et Wigner, MNBW, is a modified multi-level Breit-Wigner treatment) and psi-chi Doppler broadening. There are no normalizations done except for the cases with LSSF=1. The moments of these cross-sections are computed, and the probability tables deduced from them. The table orders will mainly depend on the required accuracy, with a maximum of 11. The probability tables for all zones and ladders are merged to get the final table for each energy group. The Gauss-quadrature mathematical principle gives those probability tables their sturdiness, allowing many utilitarian operations such as table condensation, isotope mixing, or interpolation.

In this case, TRIPOLI makes use of the probability table only in the URR of each evaluation (although some effects of the resolved range or the smooth high-energy range may affect energy groups that overlap the limits of the URR). Competitive widths are treated if they are present in this range. This leads to the generation of “statistical” resonances in the competing open channels if widths are present in File 2 of the evaluation (as in the U-238 evaluations). The normal ENDF procedure is to use the statistical results for elastic scattering, fission, and capture, but to use the smooth cross section from File 3 for the competing reaction (inelastic scattering in this case). Other CALENDF specificities include threshold broadening and the use of a cubic interpolation law for the pointwise data.

Figure 8 illustrates some features of the performance of these methods. The large oscillations in the effective cross sections are caused by using definite group bounds for

each sampling step. They gradually go away when more ladders are averaged in, and integral results should be reasonable, even with the statistical oscillations in the detailed cross sections. The effect of using self shielding for the competing inelastic reaction is seen above 50 keV, where CALENDF predicts a slightly smaller total cross section than the other methods.

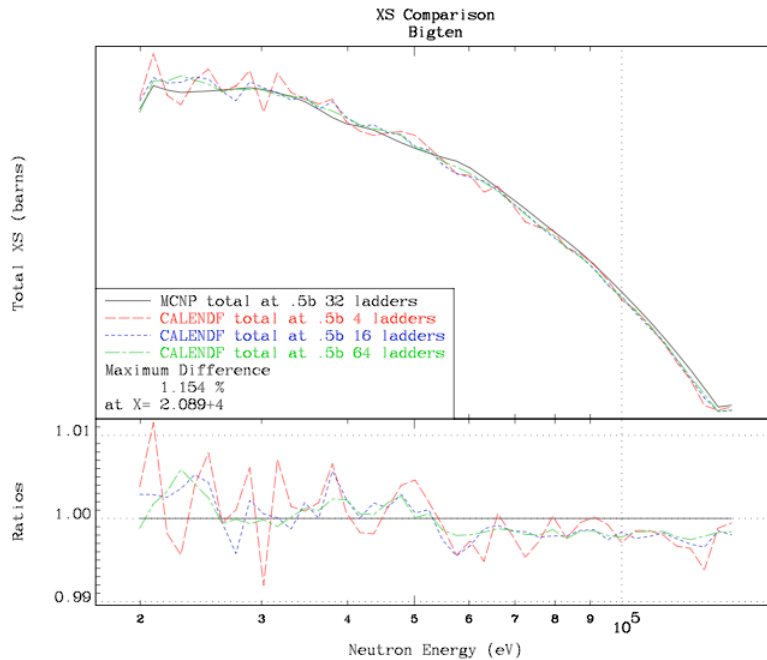


**Figure 8. Performance of the CALENDF method in the unresolved resonance range.**

Figure 9 shows the self shielding effect in the competitive inelastic channel in the unresolved energy range. This CALENDF calculation used 64 ladders. The agreement between the infinitely dilute cross section and the ENDF/B-VII value is very good, except down close to the threshold where the ENDF curve uses fairly large linearly interpolated steps. The self shielding effect is on the order of 5%. This reduction in the inelastic downscattering would be expected to lead to a higher flux in the upper part of the URR and a lower flux at lower energies, just as seen in Figure 1. The integral effect of these differences probably explains most of the difference between TRIPOLI and the other codes seen in Table 1 (roughly .05%). The ENDF/B-VII UR evaluation stops at 149 keV, which is the threshold for the second inelastic level. The formalism only allows for one competing channel. Therefore, using the self shielding effect for inelastic scattering results in some discontinuity at this point.

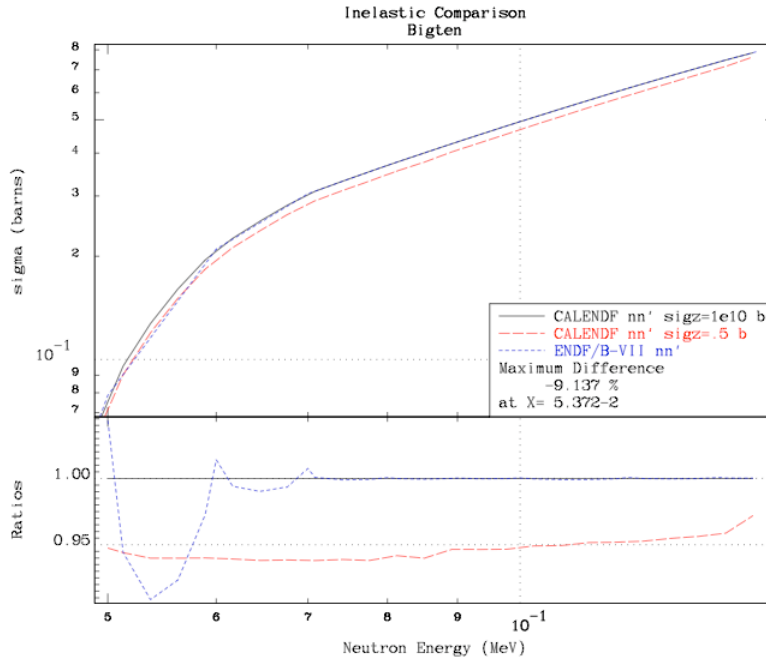


**Figure 9. Inelastic self shielding as computed by CALENDF**

**Summary of Method Used for VIM.** The VIM unresolved resonance processing code, AUROX, uses the ladder method, but using 99 pre-determined standard bins, some of which are always empty during the ladder sampling process. Cross sections are computed from the SLBW parameters and Doppler broadened with the psi-chi method. Ladder sampling continues until the statistical convergence of the resonance components of the average total, elastic, fission, and capture cross sections (2%), or when 500 ladders have been sampled. Each table is then collapsed to 20 bins whose boundaries optimize on equal probabilities. In VIM, elastic, capture, and fission cross sections are treated using conditional means, *i.e.*, a total cross section sampled from a table is associated with a set of mean partial cross sections. The LSSF parameter determines whether the cross sections sampled from the table are added to the File 3 data or used as self-shielding factors.

**Summary of Method Used for COG.** COG uses the same probability tables as MCNP.

(Note added by JCS: It seems clear from these summaries that the unresolved range processing of the same File 2 information from the evaluation based on methods that bear similar names, such as probability tables or ladders of resonances, leads to similar integral results, but the methods are far from being identical or even interchangeable. That emphasizes the importance of this unresolved range and suggests that better methodologies be derived to account for it.)

## Effects of Smoothing Energy Distributions

In a recent comparison exercise [10], some differences between TART and MCNP were traced down to the effects of the histogram distributions used in the ENDF/B-VII evaluations for the actinides. TART had chosen some time ago to ignore the lowest part of the distributions given in the ENDF file and to automatically replace the first histogram segment (say 1e-5 eV to 2 keV) with a more physically reasonable  $\sqrt{E}$  shape. MCNP, on the other hand, used the ENDF spectrum as given.

In order to determine how significant of a problem that effect might be for Bigten, we prepared some modified library files that replaced the lower few of the histogram bins with more and narrower bins on a log spacing extending down to about 40 eV. Figure 10 compares two MCNP runs: one using the normal ENDF/B-VII library, and one using the smoothed library. (Note: the other results in this report used the smoothed library).

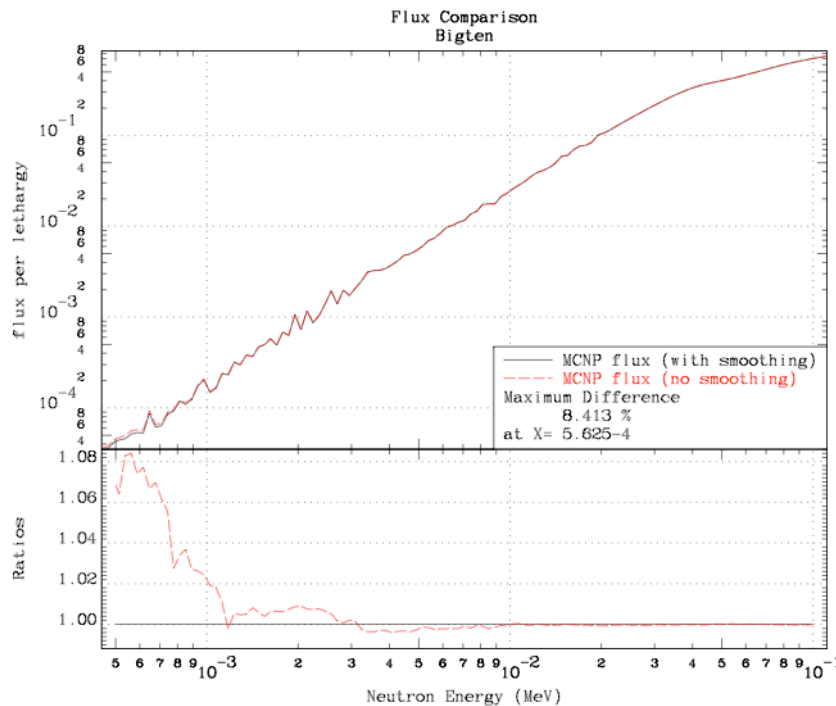


**Figure 10. Effect of not smoothing the histograms in the inelastic scattering distributions.**

Note that the effect of not smoothing the inelastic scattering distribution is negligible for the energies of interest to Bigten (energies greater than 5 keV). But at lower energies, the effect of the constant emission probability given by the histogram segment from 1e-5 eV to 1.87 keV leads to an overestimate of the flux.

Another effect highlighted in the previous comparison exercise pertains to the tabulated fission spectra for U-235 and Pu-239 in ENDF/B-VII. They are given on a fairly fine energy grid up to 10 MeV, but above there, a coarser mesh of 1 MeV steps is used. The shape of the function is very close to exponential above 10 MeV. Therefore, it is easy to smooth out the effects of the coarse grid by adding additional points between the ones given. We did this using 200 keV steps, and these modified spectra are our normal data for MCNP runs (as used in the other results quoted in this report). Figure 11 compares the effect of using the standard ENDF/B-VII library against our current smoothed library. This problem has no effect on the integral properties of Bigten, but it could be significant for a high-threshold reaction tested in the Bigten flux.

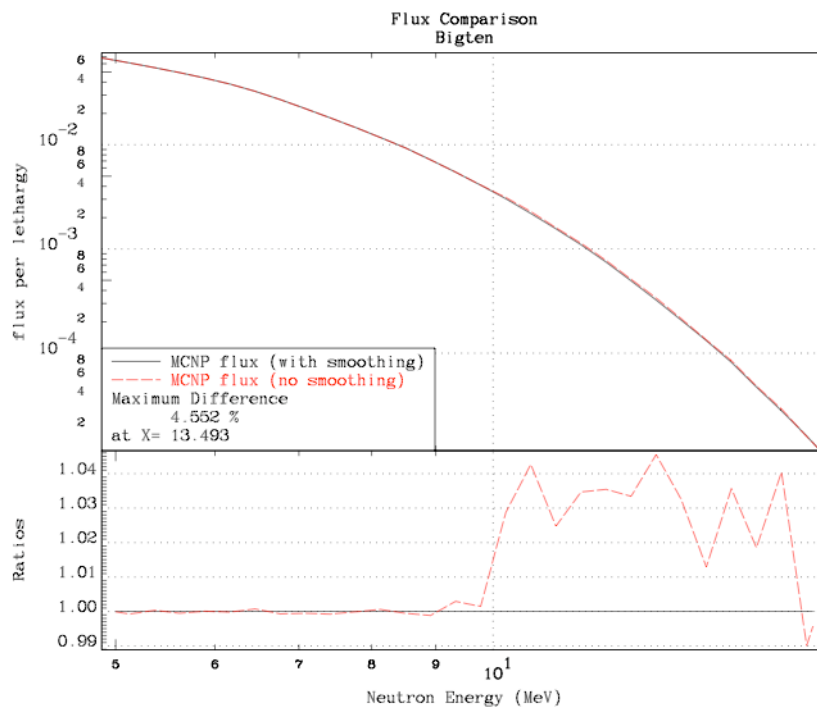


**Figure 11. Effect of the coarse energy steps above 10 MeV in the ENDF/B-VII evaluation for U-235 on Bigten.**

The behavior of all the codes at high energies is shown in Figure 12. The VIM curve was artificially cut off just above 12 MeV. It would normally continue to climb above the other curves because of an incomplete treatment of the (n,3n) reaction. This effect has no significant influence on criticality problems.

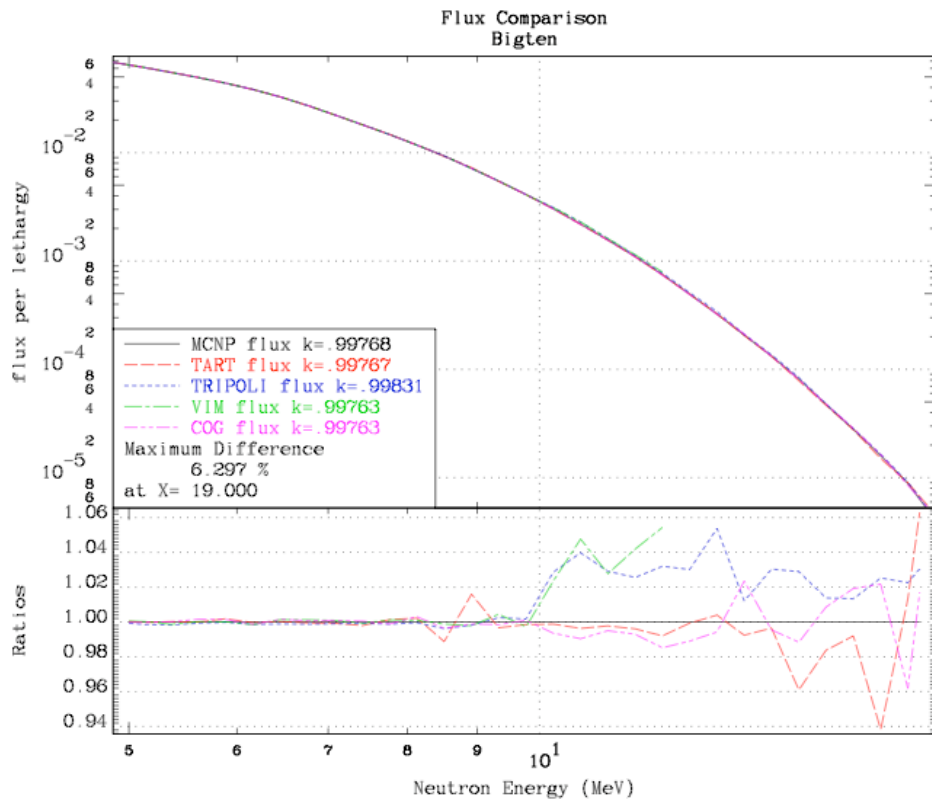


**Figure 12. Comparison of the 5 codes in the high-energy region.**

Note that MCNP, TART, and COG all use smoothing for the fission spectra above 10 MeV, but TRIPOLI and VIM do not. Both these codes can incorporate fission-spectrum smoothing by using a modified ENDF file as input. It should be stressed that the results that use smoothing are not using the official ENDF/B-VII.0 data.

## Delayed Neutron Effects

Another place that smoothing shows up is in the spectra for each time group of the delayed neutron emission. The evaluator had to approximate the emission at low energies that could not be seen in the experimental measurements [17]. This range was approximated as a Maxwellian, and the region from zero to 10 keV was approximated as a histogram segment that was an integral over this Maxwellian.

In the TART code, the author chose to represent the delayed spectra by fitting each one to a Maxwellian and to use the Maxwellian to represent the emission. Therefore, the natural shape of the region between zero and 10 keV was  $\sqrt{E}$ . There are huge percent differences between the constant histogram value and  $\sqrt{E}$  as you go down to the low energies! In order to facilitate comparisons between TART and MCNP, a modification

was made to the data processing to replace the constant value between zero and 10 keV with many smaller histogram steps on log intervals chosen to approximate  $\sqrt{E}$ . The effect of this is very small in the region of importance for the Bigten problem. The MCNP results shown in the report include this smoothing effect, but it is buried in the effects of inelastic scattering in these plots.

Another factor relating to delayed neutrons may also be found in code comparisons. Until recently, most codes emitted all fission neutrons (nubar-total) using the prompt fission spectrum. Now, many codes emit the fission neutrons using the more realistic combination of prompt and delayed spectra, what MCNP calls “natural sampling.” An option in the code allows it to be run either way. The effect of emitting both prompt and delayed neutrons using the prompt spectrum is to increase K-eff from 0.99768 to 0.99937. Figure 13 illustrates the difference in the flux between these methods as computed by MCNP.

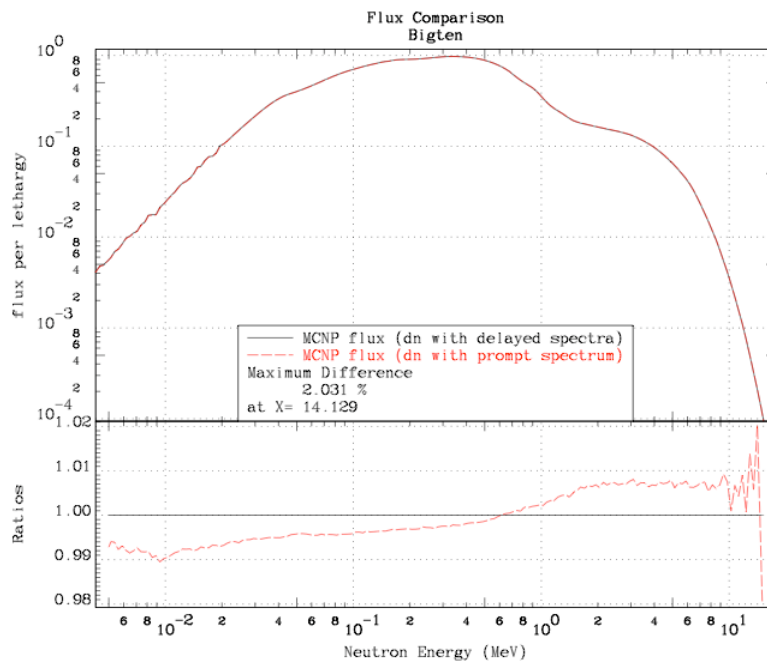


**Figure 13. Delayed-Neutron Emission Effect on Bigten Flux.**

## Effects of Interpolation for Energy Distributions

The ENDF evaluation for U-238 specifies “INT=2” for incident energy interpolation in the continuum inelastic scattering reaction (MT=91). This would normally mean that you would interpolate on incident energy between two points with the same secondary energy. However, this clearly leads to incorrect values for the upper energy limit at energies between grid points in the evaluation; that is, for E between E1 and E2, the upper limit would be the maximum energy corresponding to E2 (normally the higher one). It clearly should have some value that varies smoothly between the maximum value appropriate to E1 and the maximum value appropriate to E2. The MCNP and TART developers recognized this many years ago, and their codes ignore the specified “INT=2” interpolation law in favor of doing something more physically reasonable. This is hard-wired in these codes and cannot be overcome.

The TRIPOLI developers, on the other hand, chose to do what the ENDF evaluation says. The results of this can be seen in the TRIPOLI curves on the various graphs. ENDF allows another option for incident interpolation, called “unit-base” interpolation, which has the desired effect of interpolating more physically between E1 and E2. As a test, the entry “INT=2” in U-238 was changed to “INT=22,” and the calculation was repeated. The result is shown in Figure 14. Note that the oscillations in the MeV area are explained, and that there were also some smaller changes at low energies.

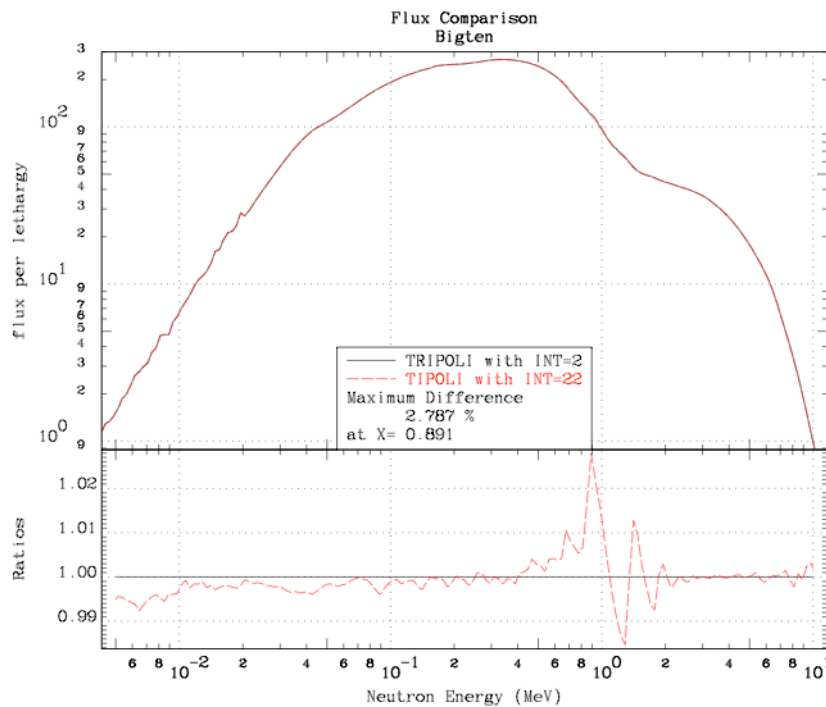


**Figure 14. Effect of different options for incident-energy interpolation in the TRIPOLI code.**

## Multigroup Results

This simple model for Bigten is readily calculated using one-dimensional Sn methods. Here is a comparison between PARTISN [18] results using data from TRANSX [19] and MCNP.

**Table 3. Comparison of Sn to MCNP for Bigten**

Quantity	TRANSX/PARTISN	MCNP
K-eff	.99768	.99724
Absorption	.876627	.876444
Leakage	.126142	.125880
Flux	60.8852	60.8755

The agreement is very good considering the many differences in methods between Sn and continuous-energy Monte Carlo. Figure 15 shows a comparison of the flux between the two methods.

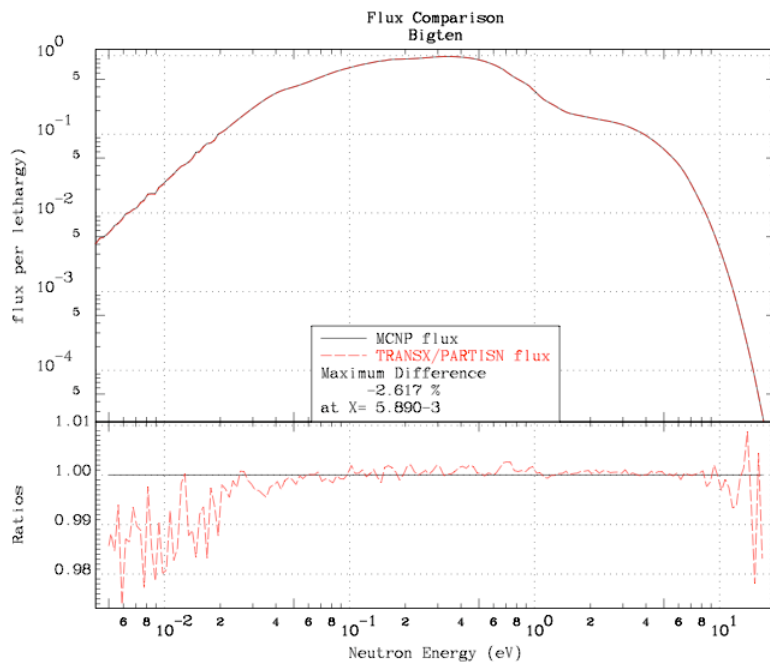


**Figure 15. Comparison of flux for Bigten between MCNP and an Sn calculation.**

The following table shows some of the central reaction rate ratios as computed by both multigroup and Monte Carlo methods for the spherical model of Bigten. The rates were computed in a central region of radius 1.5 cm. The agreement between the two methods is very good, but the agreement between calculation and experiment leaves something to be desired.

**Table 4. Central Reaction Rate Ratios**

<b>Rate Ratio</b>	<b>Experiment</b>	<b>MG C/E</b>	<b>MCNP C/E</b>
U238f/U235f	.03739+/-0.00034	.956	.954
Np237f/U235f	.3223+/-0.0039	.974	.972
U233f/U235f	1.580+/-0.030	.977	.978
Pu239f/U235f	1.1936+/-0.0084	.974	.975
U238c/U235f	.110+/-0.003	.969	.969

The TRANSX code was used to generate the self-shielded cross sections using a MATXS library generated by NJOY using 267 groups from the set of 616 and a fission spectrum weighting function. Iteration was used to improve the fission chi based on the computed flux until k-eff began to converge (about a 0.2% effect on k-eff). The PARTISN Sn calculation used P5 and S32 with 120 spatial intervals.

## Results for Other Models and Evaluation Sets

The Bigten experiment was designed to show the effects of an enrichment of approximately 10%. To obtain this, the core was made up of interleaved slabs of highly enriched and natural uranium in the appropriate ratio. The core was surrounded by a large reflector of natural uranium. The resulting assembly was closer to cylindrical than the spherical approximation discussed above. The evaluation of the Bigten experiment for the ICSBEP Handbook actually generated three models: a “detailed” model intended to include most of the complexities of the experiment, a “simplified” model that still includes the slabs and reflector in reasonable detail, and a “homogenized” model that represents the core and reflector as single materials and that uses a two-dimensional cylindrical two-region representation of Bigten. Table 4 shows results for the “simplified” and “homogenized” models using MCNP and ENDF/B-VII.

**Table 4. MCNP Results for Bigten using ICSBEP Handbook Models.**

<b>Case</b>	<b>Model K-eff</b>	<b>ENDF/B-VII C/E</b>
IMF007s	1.0045+/-0.0007	.99995+/-0.00010
IMF007h	.9948+/-0.0013	1.00005+/-0.00010

From a “data testing” point of view, these results are very satisfactory. From a “code comparison” point of view, they suggest the bias between the spherical model and the more realistic model that might be seen when comparing the results from other codes using ENDF/B-VII data and these more detailed models.

Table 5 shows results for JEFF-3.1 and JENDL-3.3 as computed by TRIPOLI-4.5 for the ICSBEP Handbook detailed, simplified, and homogenized models.

**Table 5. TRIPOLI Results for Bigten using Other Evaluations Sets**

<b>Case</b>	<b>Model K-eff</b>	<b>JEFF-3.1 C/E</b>	<b>JENDL-3.3 C/E</b>
IMF007d	1.0045+/- .0007	0.99416	1.00587
IMF007s	1.0045+/- .0007	0.99343	1.00498
IMF007h	0.9948+/- .0013	0.99347	1.00712

These results show that the difference between evaluation sets is still a bigger effect than the differences between the simulation codes for the kinds of problems exemplified by Bigten.

## **Conclusions**

The primary conclusion is that these six codes are all in agreement for calculating K-eff to within the desired target of 0.1%. These means that they are all suitable for use in analyzing assemblies similar to Bigten, and they are all useful for exploring possible improvements in the evaluated data for this range of applicability. However, this study has highlighted a number of smaller differences between the codes or the data libraries that should be understood by users.

The most important is a proper treatment of the fission spectrum, combining both prompt and delayed components. Using the older common convention of emitting all the fission neutrons (prompt and delayed) using the prompt spectrum can lead to differences larger than the 0.1% target. All these codes use the more complete “natural” method, but persons who use another code should attempt to determine how the fission spectrum is treated in that code.

With respect to the data libraries, the most important effect probably comes from how the inelastic reaction in the unresolved resonance range is treated. If it is self shielded, the flux, production, absorption, and leakage can show strong differences from the results with codes that do not self shield inelastic scattering (the normal ENDF convention). The integral effect of these differences on K-eff appears to be smaller than the 0.1% target. Additional work to explore this problem should be done by the theory and evaluation communities.

Another data effect comes from the methods used for incident-energy interpolation in the continuum distributions for neutron scattering. Here it would be desirable for the evaluations to use a unit-base interpolation procedure and to make sure that the incident-energy grids are fine enough for reasonable interpolation. Some transport codes do this automatically, but it would be more general to include this change in the evaluations. The effect of this problem on K-eff seems to be small for Bigten.

Another data issue is the possible change of histogram emission spectra to use a  $\sqrt{E}$  shape at low emission energies. Here again, some transport codes automatically make this change, but it would be more general to include the change in the evaluations. The effect of this “smoothing” on K-eff is small for Bigten.

The final data effect comes from the overly coarse energy grids used above 10 MeV for the prompt fission spectra of U-235 and Pu-239 in ENDF/B-VII and JEFF-3.1. These should be changed in the evaluations as soon as possible. Some codes attempt to patch this themselves, but it would be more general to change the evaluations. This problem does not affect the K-eff value for Bigten, but it could be important when looking at reaction rates from high-threshold reactions.

This particular study did not include all the criticality simulation codes used around the world. Other code developers and users are welcome to compare their results to these. The ultimate goal is to try to get universal agreement between the codes at the 0.1% level for K-eff calculations.

## Acknowledgements

One author (JCS) wishes to acknowledge the contributions of P. Ribon (CALENDF's real father) and Y. Peneliau (CEA).

## References

[1] “ENDF/B-VII.0: Next Generation Evaluated Nuclear Data Library for Nuclear Science and Technology”, many authors, Nuclear Data Sheets 107 (2006) pp. 2931-3060.

[2] **JEFF-3.1**. “The JEFF-3.1 Nuclear Data Library,” The JEFF Team, JEFF Report 21, NEA/OECD 6190, 2006, ISBN 92-64-02314-3.  
[http://www.nea.fr/html/dbdata/projects/nds\\_jef.htm](http://www.nea.fr/html/dbdata/projects/nds_jef.htm).

[3] **JENDL-3.3**. "Descriptive Data of JENDL-3.3 (Part I and II)", K. Shibata (Ed.), JAERI-Data/Code 2002-026 (2003). <http://www.ndc.tokai-sc.jaea.go.jp/jendl/j33/j33.html>

[4] **MCNP** - A General Monte Carlo N-Particle Transport Code, Version 5, Volume I: Overview and Theory, X-5 Monte Carlo Team, Los Alamos National Laboratory report LA-UR-03-1987 (April 24, 2003). Portions of the MCNP manual are available on-line

at <http://www-xdiv.lanl.gov/x5/MCNP/themanual.html>. The runs reported here were done using version 1.4 with a 32-bit linux binary running on a cluster of AMD processors.

[5] **TART 2005**: A Coupled Neutron-Photon 3-D, Combinatorial Geometry, Time Dependent Monte Carlo Transport Code, Report: by D.E. Cullen, November 22, 2005, Lawrence Livermore National Laboratory report UCRL-SM-218009. TART 2008 in preparation.

[6] **TRIPOLI-4.5** "Notice d'utilisation du code TRIPOLI-4 version 5: code de transport de particules par methode de Monte Carlo", F.X. Hugot, E Dumonteil, O. Petit, Y.K. Lee, C. Jouanne, A. Mazzolo, Rapport DM2S, SERMA/LTSD/RT/07-4169/A, 2007. <http://www.nea.fr/abs/html/nea-1716.html>.

[7] Status of the **VIM** Monte Carlo Neutron/Photon Transport Code, by R. N. Blomquist, Proceedings of the 12th Biennial RPSD Topical Meeting, Santa Fe, NM, April 14-18, 2002. Separate VIM User's Manual available with the code from RSICC.

[8] **COG** – A Multiparticle Monte Carlo Transport Code, User's Manual, Fifth Edition, Richard M. Buck, Edward Lent, Tom Wilcox, Stella Hadjimarkos, UCRL-TM-202590, September 1, 2002.

[9] **International Handbook of Evaluated Criticality Safety Benchmark Experiments**, Nuclear Energy Agency report NEA/NSC/DOC(55(03), Sept 2006 edition.

[10] **Criticality Calculations** Using LANL and LLNL Neutron Transport Codes, by Dermott E. Cullen (LLNL), Peter Brown (LLNL), Edward Lent (LLNL), Robert MacFarlane (LANL), and Scott McKinley (LLNL), Lawrence Livermore National Laboratory report UCRL-TR-237333, November 22, 2007.

[11] **ENDF-202**. CSEWG Benchmark Specifications, Brookhaven National Laboratory report BNL-19302 (updated September 1982).

[12] **ENDF-102**. Data Formats and Procedures for the Evaluated Nuclear Data File ENDF-6, V. McLane, ed., Brookhaven National Laboratory report BNL-NCS-44945-01/04-Rev., April 2001.

[13] "The **NJOY** Nuclear Data Processing System, Version 91," Los Alamos National Laboratory report LA-12740-M, by R. E. MacFarlane and D. W. Muir, (October 1994). For latest information, see <http://t2.lanl.gov/codes/njoy99>.

[14] ] "CALENDF-2005: User manual", J-Ch. Sublet, P. Ribon and M. Coste-Delclaux, CEA-R-6131, ISSN 0429-3460, 2006. <http://www.nea.fr/abs/html/nea-1278.html>

[15] Dermott E. Cullen, "PREPRO 2007: 2007 ENDF/B pre-processing Codes", IAEA-NDS-39, Rev. 13, March 17, 2007, Nuclear Data Section, International Atomic Energy Agency, Vienna, Austria.

[16] Dermott E. Cullen, "Nuclear Cross Section Processing", Handbook of Nuclear Reactor Calculation, vol. I, Yigal Ronen, Editor, CRC Press, inc., Boca Raton, Florida (1986).

[17] "Evaluation and Application of Delayed Neutron Precursor Data," by Michaela Clarice Brady, Los Alamos National Laboratory report LA-11534-T, April 1989.

[18] **PARTISN**. "PARTISN: A Time-Dependent, Parallel Neutral Particle Transport Code System," by Ray E. Alcouffe, Randal S. Baker, Jon A. Dahl, Scott A. Turner, and Robert C. Ward, Los Alamos National Laboratory report LA-UR-05-3925, revised May 2005.

[19] **TRANSX**, "TRANSX2: A Code for Interfacing MATXS Cross-Section Libraries to Nuclear Transport Codes," by R. E. MacFarlane, Los Alamos National Laboratory report LA-12312-MS, July 1992. Also see <http://t2.lanl.gov/codes/transx>, <http://t2.lanl.gov/publications/transx.ps>, and <http://t2.lanl.gov/codes/transx-hyper/TRANSX.html>.

## Appendix

Here are the boundaries of the 616 groups suggested for tallying differential results for this study. As an alternative, the 256 groups above 100 eV can be used, because Bigten has no significant contribution from the thermal region.

1.00000E-11	1.04713E-11	1.09648E-11	1.14815E-11	1.20226E-11
1.25893E-11	1.31826E-11	1.38038E-11	1.44544E-11	1.51356E-11
1.58489E-11	1.65959E-11	1.73780E-11	1.81970E-11	1.90546E-11
1.99526E-11	2.08930E-11	2.18776E-11	2.29087E-11	2.39883E-11
2.51189E-11	2.63027E-11	2.75423E-11	2.88403E-11	3.01995E-11
3.16228E-11	3.31131E-11	3.46737E-11	3.63078E-11	3.80189E-11
3.98107E-11	4.16869E-11	4.36516E-11	4.57088E-11	4.78630E-11
5.01187E-11	5.24807E-11	5.49541E-11	5.75440E-11	6.02560E-11
6.30957E-11	6.60693E-11	6.91831E-11	7.24436E-11	7.58578E-11
7.94328E-11	8.31764E-11	8.70964E-11	9.12011E-11	9.54993E-11
1.00000E-10	1.04713E-10	1.09648E-10	1.14815E-10	1.20226E-10
1.25893E-10	1.31826E-10	1.38038E-10	1.44544E-10	1.51356E-10
1.58489E-10	1.65959E-10	1.73780E-10	1.81970E-10	1.90546E-10
1.99526E-10	2.08930E-10	2.18776E-10	2.29087E-10	2.39883E-10
2.51189E-10	2.63027E-10	2.75423E-10	2.88403E-10	3.01995E-10
3.16228E-10	3.31131E-10	3.46737E-10	3.63078E-10	3.80189E-10
3.98107E-10	4.16869E-10	4.36516E-10	4.57088E-10	4.78630E-10
5.01187E-10	5.24807E-10	5.49541E-10	5.75440E-10	6.02560E-10
6.30957E-10	6.60693E-10	6.91831E-10	7.24436E-10	7.58578E-10
7.94328E-10	8.31764E-10	8.70964E-10	9.12011E-10	9.54993E-10
1.00000E-09	1.04713E-09	1.09648E-09	1.14815E-09	1.20226E-09

1.25893E-09 1.31826E-09 1.38038E-09 1.44544E-09 1.51356E-09  
1.58489E-09 1.65959E-09 1.73780E-09 1.81970E-09 1.90546E-09  
1.99526E-09 2.08930E-09 2.18776E-09 2.29087E-09 2.39883E-09  
2.51189E-09 2.63027E-09 2.75423E-09 2.88403E-09 3.01995E-09  
3.16228E-09 3.31131E-09 3.46737E-09 3.63078E-09 3.80189E-09  
3.98107E-09 4.16869E-09 4.36516E-09 4.57088E-09 4.78630E-09  
5.01187E-09 5.24807E-09 5.49541E-09 5.75440E-09 6.02560E-09  
6.30957E-09 6.60693E-09 6.91831E-09 7.24436E-09 7.58578E-09  
7.94328E-09 8.31764E-09 8.70964E-09 9.12011E-09 9.54993E-09  
1.00000E-08 1.04713E-08 1.09648E-08 1.14815E-08 1.20226E-08  
1.25893E-08 1.31826E-08 1.38038E-08 1.44544E-08 1.51356E-08  
1.58489E-08 1.65959E-08 1.73780E-08 1.81970E-08 1.90546E-08  
1.99526E-08 2.08930E-08 2.18776E-08 2.29087E-08 2.39883E-08  
2.51189E-08 2.63027E-08 2.75423E-08 2.88403E-08 3.01995E-08  
3.16228E-08 3.31131E-08 3.46737E-08 3.63078E-08 3.80189E-08  
3.98107E-08 4.16869E-08 4.36516E-08 4.57088E-08 4.78630E-08  
5.01187E-08 5.24807E-08 5.49541E-08 5.75440E-08 6.02560E-08  
6.30957E-08 6.60693E-08 6.91831E-08 7.24436E-08 7.58578E-08  
7.94328E-08 8.31764E-08 8.70964E-08 9.12011E-08 9.54993E-08  
1.00000E-07 1.04713E-07 1.09648E-07 1.14815E-07 1.20226E-07  
1.25893E-07 1.31826E-07 1.38038E-07 1.44544E-07 1.51356E-07  
1.58489E-07 1.65959E-07 1.73780E-07 1.81970E-07 1.90546E-07  
1.99526E-07 2.08930E-07 2.18776E-07 2.29087E-07 2.39883E-07  
2.51189E-07 2.63027E-07 2.75423E-07 2.88403E-07 3.01995E-07  
3.16228E-07 3.31131E-07 3.46737E-07 3.63078E-07 3.80189E-07  
3.98107E-07 4.16869E-07 4.36516E-07 4.57088E-07 4.78630E-07  
5.01187E-07 5.24807E-07 5.49541E-07 5.75440E-07 6.02560E-07  
6.30957E-07 6.60693E-07 6.91831E-07 7.24436E-07 7.58578E-07  
7.94328E-07 8.31764E-07 8.70964E-07 9.12011E-07 9.54993E-07  
1.00000E-06 1.04713E-06 1.09648E-06 1.14815E-06 1.20226E-06  
1.25893E-06 1.31826E-06 1.38038E-06 1.44544E-06 1.51356E-06  
1.58489E-06 1.65959E-06 1.73780E-06 1.81970E-06 1.90546E-06  
1.99526E-06 2.08930E-06 2.18776E-06 2.29087E-06 2.39883E-06  
2.51189E-06 2.63027E-06 2.75423E-06 2.88403E-06 3.01995E-06  
3.16228E-06 3.31131E-06 3.46737E-06 3.63078E-06 3.80189E-06  
3.98107E-06 4.16869E-06 4.36516E-06 4.57088E-06 4.78630E-06  
5.01187E-06 5.24807E-06 5.49541E-06 5.75440E-06 6.02560E-06  
6.30957E-06 6.60693E-06 6.91831E-06 7.24436E-06 7.58578E-06  
7.94328E-06 8.31764E-06 8.70964E-06 9.12011E-06 9.54993E-06  
1.00000E-05 1.04713E-05 1.09648E-05 1.14815E-05 1.20226E-05  
1.25893E-05 1.31826E-05 1.38038E-05 1.44544E-05 1.51356E-05  
1.58489E-05 1.65959E-05 1.73780E-05 1.81970E-05 1.90546E-05  
1.99526E-05 2.08930E-05 2.18776E-05 2.29087E-05 2.39883E-05  
2.51189E-05 2.63027E-05 2.75423E-05 2.88403E-05 3.01995E-05  
3.16228E-05 3.31131E-05 3.46737E-05 3.63078E-05 3.80189E-05  
3.98107E-05 4.16869E-05 4.36516E-05 4.57088E-05 4.78630E-05  
5.01187E-05 5.24807E-05 5.49541E-05 5.75440E-05 6.02560E-05  
6.30957E-05 6.60693E-05 6.91831E-05 7.24436E-05 7.58578E-05  
7.94328E-05 8.31764E-05 8.70964E-05 9.12011E-05 9.54993E-05  
1.00000E-04 1.04713E-04 1.09648E-04 1.14815E-04 1.20226E-04  
1.25893E-04 1.31826E-04 1.38038E-04 1.44544E-04 1.51356E-04  
1.58489E-04 1.65959E-04 1.73780E-04 1.81970E-04 1.90546E-04  
1.99526E-04 2.08930E-04 2.18776E-04 2.29087E-04 2.39883E-04  
2.51189E-04 2.63027E-04 2.75423E-04 2.88403E-04 3.01995E-04  
3.16228E-04 3.31131E-04 3.46737E-04 3.63078E-04 3.80189E-04  
3.98107E-04 4.16869E-04 4.36516E-04 4.57088E-04 4.78630E-04  
5.01187E-04 5.24807E-04 5.49541E-04 5.75440E-04 6.02560E-04  
6.30957E-04 6.60693E-04 6.91831E-04 7.24436E-04 7.58578E-04

7.94328E-04 8.31764E-04 8.70964E-04 9.12011E-04 9.54993E-04  
1.00000E-03 1.04713E-03 1.09648E-03 1.14815E-03 1.20226E-03  
1.25893E-03 1.31826E-03 1.38038E-03 1.44544E-03 1.51356E-03  
1.58489E-03 1.65959E-03 1.73780E-03 1.81970E-03 1.90546E-03  
1.99526E-03 2.08930E-03 2.18776E-03 2.29087E-03 2.39883E-03  
2.51189E-03 2.63027E-03 2.75423E-03 2.88403E-03 3.01995E-03  
3.16228E-03 3.31131E-03 3.46737E-03 3.63078E-03 3.80189E-03  
3.98107E-03 4.16869E-03 4.36516E-03 4.57088E-03 4.78630E-03  
5.01187E-03 5.24807E-03 5.49541E-03 5.75440E-03 6.02560E-03  
6.30957E-03 6.60693E-03 6.91831E-03 7.24436E-03 7.58578E-03  
7.94328E-03 8.31764E-03 8.70964E-03 9.12011E-03 9.54993E-03  
1.00000E-02 1.04713E-02 1.09648E-02 1.14815E-02 1.20226E-02  
1.25893E-02 1.31826E-02 1.38038E-02 1.44544E-02 1.51356E-02  
1.58489E-02 1.65959E-02 1.73780E-02 1.81970E-02 1.90546E-02  
1.99526E-02 2.08930E-02 2.18776E-02 2.29087E-02 2.39883E-02  
2.51189E-02 2.63027E-02 2.75423E-02 2.88403E-02 3.01995E-02  
3.16228E-02 3.31131E-02 3.46737E-02 3.63078E-02 3.80189E-02  
3.98107E-02 4.16869E-02 4.36516E-02 4.57088E-02 4.78630E-02  
5.01187E-02 5.24807E-02 5.49541E-02 5.75440E-02 6.02560E-02  
6.30957E-02 6.60693E-02 6.91831E-02 7.24436E-02 7.58578E-02  
7.94328E-02 8.31764E-02 8.70964E-02 9.12011E-02 9.54993E-02  
1.00000E-01 1.04713E-01 1.09648E-01 1.14815E-01 1.20226E-01  
1.25893E-01 1.31826E-01 1.38038E-01 1.44544E-01 1.51356E-01  
1.58489E-01 1.65959E-01 1.73780E-01 1.81970E-01 1.90546E-01  
1.99526E-01 2.08930E-01 2.18776E-01 2.29087E-01 2.39883E-01  
2.51189E-01 2.63027E-01 2.75423E-01 2.88403E-01 3.01995E-01  
3.16228E-01 3.31131E-01 3.46737E-01 3.63078E-01 3.80189E-01  
3.98107E-01 4.16869E-01 4.36516E-01 4.57088E-01 4.78630E-01  
5.01187E-01 5.24807E-01 5.49541E-01 5.75440E-01 6.02560E-01  
6.30957E-01 6.60693E-01 6.91831E-01 7.24436E-01 7.58578E-01  
7.94328E-01 8.31764E-01 8.70964E-01 9.12011E-01 9.54993E-01  
1.00000E+00 1.04713E+00 1.09648E+00 1.14815E+00 1.20226E+00  
1.25893E+00 1.31826E+00 1.38038E+00 1.44544E+00 1.51356E+00  
1.58489E+00 1.65959E+00 1.73780E+00 1.81970E+00 1.90546E+00  
1.99526E+00 2.08930E+00 2.18776E+00 2.29087E+00 2.39883E+00  
2.51189E+00 2.63027E+00 2.75423E+00 2.88403E+00 3.01995E+00  
3.16228E+00 3.31131E+00 3.46737E+00 3.63078E+00 3.80189E+00  
3.98107E+00 4.16869E+00 4.36516E+00 4.57088E+00 4.78630E+00  
5.01187E+00 5.24807E+00 5.49541E+00 5.75440E+00 6.02560E+00  
6.30957E+00 6.60693E+00 6.91831E+00 7.24436E+00 7.58578E+00  
7.94328E+00 8.31764E+00 8.70964E+00 9.12011E+00 9.54993E+00  
1.00000E+01 1.04713E+01 1.09648E+01 1.14815E+01 1.20226E+01  
1.25893E+01 1.31826E+01 1.38038E+01 1.44544E+01 1.51356E+01  
1.58489E+01 1.65959E+01 1.73780E+01 1.81970E+01 1.90546E+01  
1.99526E+01 2.00000E+01